Time-resolved crystallography of ultrafast light driven DNA repair by photolyases

Photolyase is an enzyme that repairs DNA lesions caused by ultraviolet (UV) exposure, such as cyclobutane pyrimidine dimers (CPDs), in which the C5 and C6 carbons of one pyrimidine base covalently bond with the C5' and C6' carbons of an adjacent base [1] (Fig. 1). The catalytic process of CPD photolyases involves multiple redox reactions. The enzyme is first activated through the photoreduction of its coenzyme, flavin adenine dinucleotide (FAD), from its oxidized form (FAD_{ox}) to its reduced form ($FADH^-$) [2]. This photoreduction process requires two single-electron transfer steps, mediated by an electron transfer chain that includes three tryptophan residues.

We employed time-resolved serial femtosecond crystallography (TR-SFX) to elucidate the structural mechanism underlying the photoreduction processes in the *Methanosarcina mazei* class II CPD photolyase (*Mm*CPDII) [3]. Our analysis revealed an Asn/Arg-Asp redox sensor triad that regulates FAD rehybridization and protonation. Additionally, we observed buckling and twisting of the isoalloxazine ring of the coenzyme FAD, occurring within the submicrosecond regime following the light-triggered electron transfer step [3]. This TR-SFX investigation of the photoreduction process provided a foundation for studying the main function of the *Mm*CPDII photolyase—the repair of CPD lesions. We further elucidated the dynamic structural mechanisms of DNA repair through time-resolved crystallographic analyses conducted at the X-ray free electron laser (XFEL) facilities, SACLA **BL2** and SwissFEL Alvra.

Crystals of enzyme-DNA complexes in the pre-reaction state were grown under dark and anaerobic conditions by mixing reduced photolyase with damaged DNA [4,5]. Blue light, which triggers the reaction, was applied to the crystals, followed by XFEL irradiation at time intervals ranging from picoseconds to sub-milliseconds, to capture diffraction patterns [5]. By analyzing tens of thousands of diffraction images, we reconstructed the three-dimensional structures of the enzyme and DNA during the repair process as a series of snapshots.

Two series of TR-SFX experiments were conducted: one from picoseconds (ps) to nanoseconds (ns), and the other from nanoseconds to microseconds (μs) [5]. The CPD repair begins at 100 ps, with Arg256 (R256) becoming dynamic and moving to stabilize the CPD. This suggests the initiation of the forward electron transfer from the $FADH^-$ to the CPD (Figs. 2 and 3). By 650 picoseconds (ps), the C5–C5' bond of the CPD is predominantly split, and by 1 ns, the C6–C6' bond is also split (Fig. 3). During the following 500 ns, R256, a five-water cluster (5WC), and the $FADH^-$ coenzyme gradually return to their respective resting-state conformations. The repaired thymine bases remain within the active site during this time and begin to reanneal with the dsDNA in the microsecond range. The structures captured at 200 μs show the coexistence of a back-flipping intermediate and the reannealed product, prior to their final release from the enzyme (Fig. 3).

Overall, our results reveal the atomic mechanism by which DNA photolyases repair DNA in real time. The time-resolved intermediate structures illustrate a sequential process involving the ordered cleavage of covalent bonds, the opening of the cyclobutane ring, and the release of repaired pyrimidine bases from the enzyme, ultimately restoring the DNA double helix. DNA damage disrupts replication and transcription, leading to cellular consequences such as cell death, mutations, and carcinogenesis. This study enhances our understanding of DNA repair processes that mitigate damage linked to diseases, and is expected to accelerate the rational design of artificial enzymes and drugs using sequential structural information.

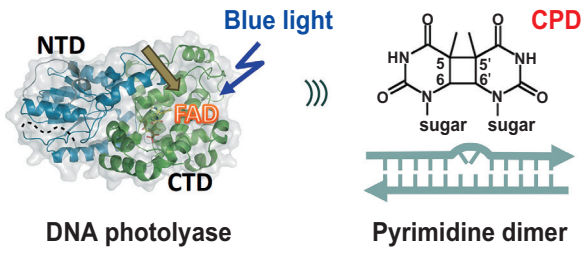

Fig. 1. Light-driven enzymatic catalysis of DNA repair by DNA photolyase. The FAD cofactor, located within the conserved folded structure of photolyase, should be fully reduced through photoreduction by the same blue light, prior to the DNA repair reaction.

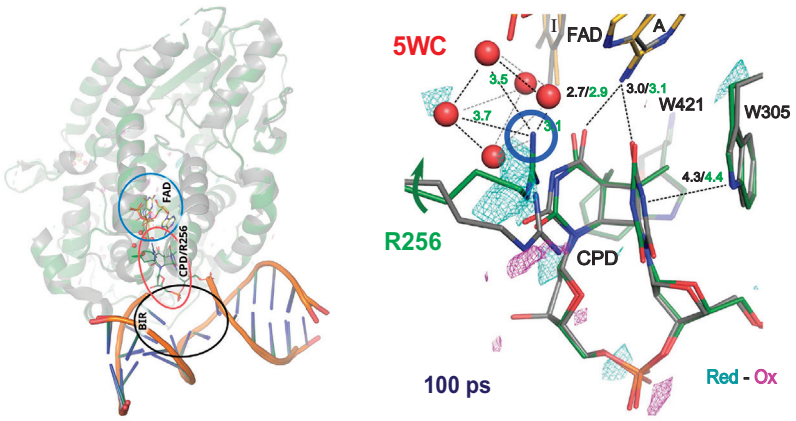

Fig. 2. *Mm*CPDII structure complexed with damaged DNA. The left panel shows the global structure, highlighting the overall fold, with the bound DNA backbone in orange. The right panel focuses on the 5WC/R256 locus in the active site at 100 ps. Interactions between the CPD; FAD and active-site residues R256, W305, and W421; and the 5WC that exclusively appears in the dark state (gray) are also depicted. In the presence of the 5WC, R256 undergoes a conformational change, with its guanidinium moiety forming the final vertex of the bipyramidal 5WC. Selected interatomic distances are indicated by dashed lines, with corresponding values in angstroms labeled nearby. [5]

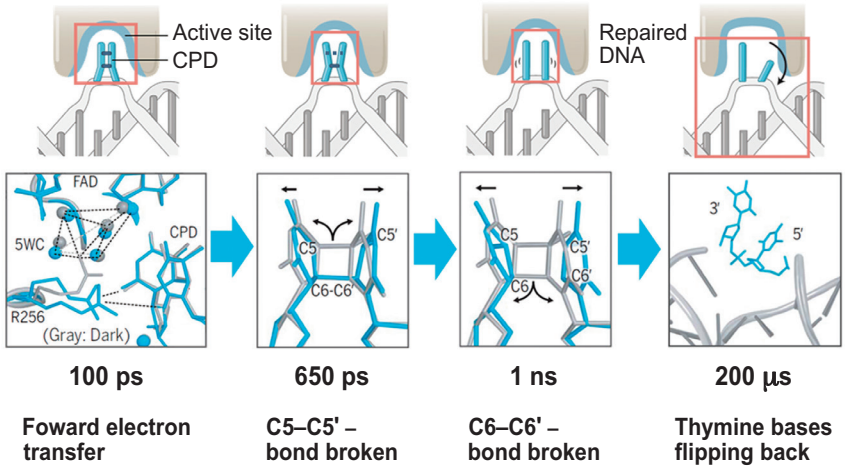

Fig. 3. Intermediates in photolyase-mediated DNA repair. The reaction is initiated by an electron transfer from the FAD cofactor embedded within the enzyme to the CPD. DNA repair by photolyase begins 100 ps after blue light irradiation. The C5–C5' bond is cleaved 650 ps after the reaction starts, followed by the cleavage of the C6–C6' bond 1 ns later. The repaired pyrimidine bases then rotate sequentially and exit the enzyme's active site, ultimately restoring the DNA double-helix structure. This last process takes approximately 200 µs, a relatively long time, and represents the rate-limiting step in the sequential enzymatic reaction. [5]

Y. Bessho[a,b,*], M. Maestre-Reyna[a,c], L.-O. Essen[d] and M.-D. Tsai[a]

[a] Institute of Biological Chemistry, Academia Sinica, Taiwan
[b] RIKEN SPring-8 Center
[c] Dept. Chemistry, National Taiwan University, Taiwan
[d] Dept. Chemistry, Philipps University Marburg, Germany

*Email: bessho@spring8.or.jp

References

[1] A. Sancar: Angew. Chem. Int. Ed. (Nobel Lecture) **55** (2016) 8502.
[2] K. Brettel and M. Byrdin: Curr. Opin. Struct. Biol. **20** (2010) 693.
[3] M. Maestre-Reyna *et al.*: Nat. Chem. **14** (2022) 677.
[4] M. Maestre-Reyna *et al.*: IUCrJ **5** (2018) 608.
[5] *M. Maestre-Reyna, P.-H. Wang, E. Nango, Y. Hosokawa, M. Saft, A. Furrer, C.-H. Yang, E. P. G. N. Putu, W.-J. Wu, H.-J. Emmerich, N. Caramello, S. Franz-Badur, C. Yang, S. Engilberge, M. Wranik, H. L. Glover, T. Weinert, H.-Y. Wu, C.-C. Lee, W.-C. Huang, K.-F. Huang, Y.-K. Chang, J.-H. Liao, J.-H. Weng, W. Gad, C.-W. Chang, A. H. Pang, K.-C. Yang, W.-T. Lin, Y.-C. Chang, D. Gashi, E. Beale, D. Ozerov, K. Nass, G. Knopp, P. J. M. Johnson, C. Cirelli, C. Milne, C. Bacellar, M. Sugahara, S. Owada, Y. Joti, A. Yamashita, R. Tanaka, T. Tanaka, F. Luo, K. Tono, W. Zarzycka, P. Müller, M. A. Alahmad, F. Bezold, V. Fuchs, P. Gnau, S. Kiontke, L. Korf, V. Reithofer, C. J. Rosner, E. M. Seiler, M. Watad, L. Werel, R. Spadaccini, J. Yamamoto, S. Iwata, D. Zhong, J. Standfuss, A. Royant, Y. Bessho, L.-O. Essen, M.-D. Tsai: Science **382** (2023) eadd7795.*